The Effect of Directionality on Northern North Sea Extreme Wave Design Criteria

Kevin Ewans
Shell International Exploration and Production,
P.O. Box 60,
2280 AB Rijswijk, The Netherlands
e-mail: kevin.ewans@shell.com

Philip Jonathan
Shell Technology Centre Thornton,
P.O. Box 1,
Chester, Chesire CH1 3SH, UK
e-mail: philip.jonathan@shell.com

The characteristics of hindcast data for extreme storms at a Northern North Sea location are shown to depend on storm direction, reflecting storm strength and fetch variability. Storm peak H_S over threshold is modeled using a generalized Pareto distribution, the parameters of which are allowed to vary smoothly with direction using a Fourier form. A directionally varying extreme value threshold is incorporated. The degree of smoothness of extreme value shape and scale with direction is regulated by roughness-penalized maximum likelihood, the optimal value of roughness selected by cross-validation. The characteristics of a 100-year storm peak H_S, estimated using the directional model, differ from those estimated when ignoring the directionality of storms. In particular, the extreme right-hand tail of omnidirectional H_{S100} is longer using the directional model, indicating in this case that ignoring directionality causes underestimation of design criteria. Although storm peak data alone are used for extreme value modeling, the influence of a storm, in directional design sectors other than that containing its storm peak direction, is incorporated by estimating the storm's directional dissipation directly from the data. An automated approach to selection of directional design sectors is described. Directional design criteria are developed using three different approaches, all consistent with an omnidirectional storm peak H_S nonexceedence probability of 0.5. We suggest a risk-cost criterion, which minimizes design cost for a given omnidirectional design specification, as an objective basis for optimal selection of directional criteria.
[DOI: 10.1115/1.2960859]

1 Introduction

Environmental design criteria for offshore facilities have inherent uncertainties and dependencies. These can be functions of climate variability in time and space, and of storm direction and track. The quality of estimation of design criteria is further dependent on data quality and sample size for extreme value modeling.

In a recent study [1], application of generalized Pareto (GPD) modeling to estimation of North Sea storm severity was reported for storms with return periods of 100–500 years based on NESS hindcast data. Uncertainty of estimates was quantified using a bootstrapping approach. Site averaging can be used to increase the sample size for modeling, and to account for randomness of storm track, in hurricane-dominated regions [2]. However, data from relatively largely separated locations are often found to be highly correlated. Thus careful quantification of uncertainty of parameter estimates and extreme quantiles is necessary, accommodating this dependency structure. For example, a bootstrapping approach has been adopted [3] to calculate interval estimates for GPD model parameters and extreme quantiles to account for spatial dependence of extremes when site averaging is used.

Extreme value modeling has a rich literature [4,5]. Of particular relevance to the current work, extremal properties of wind speeds have been modeled [6] as a function of their direction, accounting during fitting for angular dependency structure, by inflating standard errors for parameter estimates. A Fourier model has been applied [7] to characterize the extremal behavior of sea currents. A Bayesian approach has been adopted [8] using data from multiple locations. Spatial models for extremes [9,10] have also been used, as have models [11,12] for estimation of predictive distributions, which incorporate uncertainties in model parameters.

In hurricane-dominated regions (e.g., Gulf of Mexico) and regions where extratropical storms prevail (e.g., Northern North Sea), the extremal properties of storms are highly dependent on storm direction. It is important [13] to accommodate the directionality of sea states when developing design criteria for such environments. Omnidirectional extreme values derived from a directional extreme value model are different in general from those obtained from a direction-independent derivation, which ignores the distributional variability of extremes with direction. When the directional dependence of storms is modeled carefully, the distribution of an omnidirectional extreme is likely to be heavier tailed than the corresponding distribution derived from a direction-independent approach, indicating that extreme storms are more likely than we might anticipate were we to base our beliefs on models that ignore directionality. Sea state design criteria for offshore facilities are frequently provided by direction, to optimize engineering facilities for the directional environment. Debate continues [14] regarding how these should be derived in a consistent way. The current authors [13,15] present a method for developing criteria in a directional environment and apply the model to Gulf of Mexico hindcast data. A GPD is used to characterize extremal behavior, the parameters of which are allowed to vary with storm direction. The model is used to estimate distributional properties of a 100-year storm peak significant wave height and estimate self-consistent design criteria under various scenarios.

In this paper we extend the earlier model [13], applying the resulting approach to Northern North Sea hindcast data. The technical enhancements are motivated by Northern North Sea (NNS) application, and include adoption of a threshold for extreme values, which varies with storm direction, introduction of a roughness-penalized approach to maximum likelihood estimation of model parameters, and selection of the optimal model using cross-validation.

This paper is arranged as follows. In Sec. 2, we introduce the

Contributed by the Ocean Offshore and Arctic Engineering Division of ASME for publication in the JOURNAL OF OFFSHORE MECHANICS AND ARCTIC ENGINEERING. Manuscript received July 3, 2007; final manuscript received October 22, 2007; published online October 1, 2008. Assoc. Editor Elzbieta Maria Bitner-Gregersen. Paper presented at The 26th International Conference on Offshore Mechanics and Arctic Engineering (OMAE2007), San Diego, CA, June 10–15, 2007.

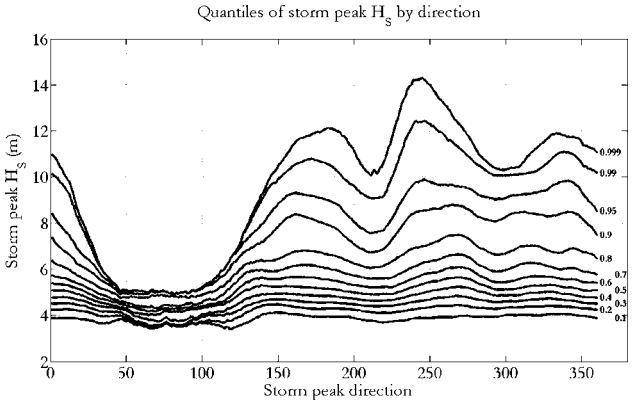

Fig. 1 Estimated quantiles of H_S^{sp} as a function of storm peak direction aggregated over all locations. Nonexceedence probabilities are given on the right-hand side.

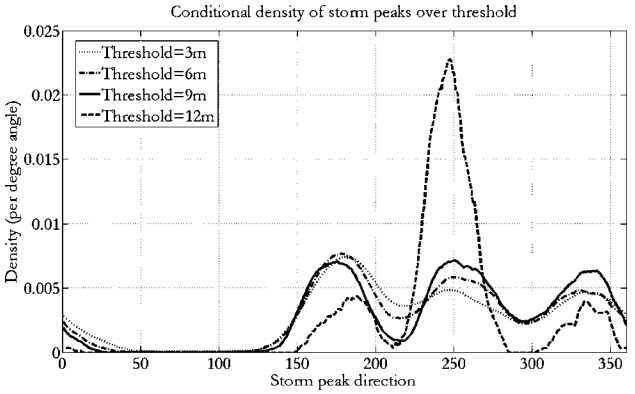

Fig. 2 Estimated densities of H_S^{sp} over threshold aggregated over all locations. Thresholds of 3 m, 6 m, 9 m, and 12 m are used.

NNS hindcast data motivating the investigation, illustrating the strong interdependency of the 100 locations considered in terms of both storm severity and direction. In Sec. 3, we introduce the extreme value model and describe the method used to estimate the variable extremal threshold. We also describe the directional model for the extreme value parameters, and outline the application of roughness-penalized maximum likelihood for parameter estimation and estimation of parameter uncertainty. In Sec. 4, we discuss the selection of directional design sectors and present a simple approach for automated sector specification based on maximizing within-sector extremal homogeneity. We then use the selected extremal model to estimate design criteria for the NNS location under different design scenarios. In Sec. 5, we summarize our findings and make suggestions for further work.

2 Data

The data examined are significant wave height H_S values from a Northern North Sea hindcast [16] for the period Oct. 1964–Sept. 1998 inclusive, sampled at 3 h intervals for winter periods until the winter of 1988, and continuously thereafter. Hindcast data have been validated against recent platform measurements [16]. For an approximate location of (2°Lng, 61°Ltt), we selected 100 grid points covering a region of approximately (5° Lng, 3° Ltt). For each storm and location, we isolated the storm peak significant wave heights H_S^{sp} and the corresponding wave direction at storm peak, henceforth referred to as storm peak direction. The procedure used to isolate H_S^{sp} was as follows: (i) a storm threshold of 4 m was selected, (ii) time intervals corresponding to storm periods were isolated as up- and down-crossings of the threshold for the median H_S profile over all locations, (iii) peaks for each storm for each location were selected as maxima of H_S within the corresponding storm period, together with corresponding storm peak (wave) direction, and (iv) storm periods for which storm peaks were found to be less that 24 h apart were merged. Finally, the sensitivity of resulting storm peak data to choice of threshold and minimum interstorm period was explored and found to be reasonable. In Step (ii), the median H_S profile was estimated, time point by time point, as the median value of H_S across all 100 locations.

Figure 1 shows estimated quantiles of H_S^{sp} as a function of storm peak direction aggregated over all locations, with storm peak direction defined clockwise from the North. Fetch-limited directions associated with land shadows are clear from the figure. For example, the shadow of Norway corresponds approximately to the interval [40,140), and the shadows of the UK and Iceland approximately to [200,230) and [280,310), respectively. The intervals [140,200), [230,280), and [310,40), respectively, correspond approximately to the long-fetch sectors of the North Sea, the Atlantic, and the Norwegian Sea/Arctic Ocean. It is also clear that the most severe storms emanate from the Atlantic at approximately 250 deg. The extremal behavior at these locations shows material directional dependence. Figure 2 gives estimates for the density of H_S^{sp} for values over thresholds of 3 m, 6 m, 9 m, and 12 m. The densities are similar for all but the largest threshold, for which the density is strongly peaked at approximately 250 deg, indicating that the storms with the largest H_S^{sp} are associated with this direction, consistent with Fig. 1.

To illustrate location interdependence with respect to both H_S^{sp} and storm peak direction, the four corner locations (referred to as NE, NW, SW, and SE) and the center location (referred to as C) were selected for further illustrations. Figure 3 gives the rank correlation of H_S^{sp} between pairs of locations for all storm peaks. All locations are strongly interdependent, the extent of the dependency decreasing with increasing distance between locations. Figure 4 is a scatter plot of H_S^{sp} for the NE and SW locations, which are the least interdependent.

Figure 5 gives median values of differences in storm peak directions for all pairs of locations from NE, NW, SW, SE, and C. The biggest angular difference is approximately 20 deg suggesting that storm peak directions are also strongly interdependent. Figure 6 is a scatter plot of storm peak direction for the NE and SW locations, which show the largest angular difference.

We note that whereas storm peaks have a unique associated storm peak direction, storms themselves do not correspond to a single direction only. Indeed, storm events extend over a wide

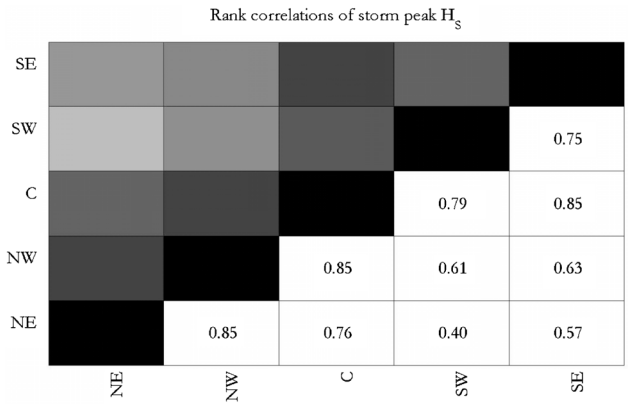

Fig. 3 Rank correlations between corner and center locations. The top left illustrates interdependence on gray-scale (black =highest, white=lowest). The bottom right gives numeric values for rank correlations between pairs of locations.

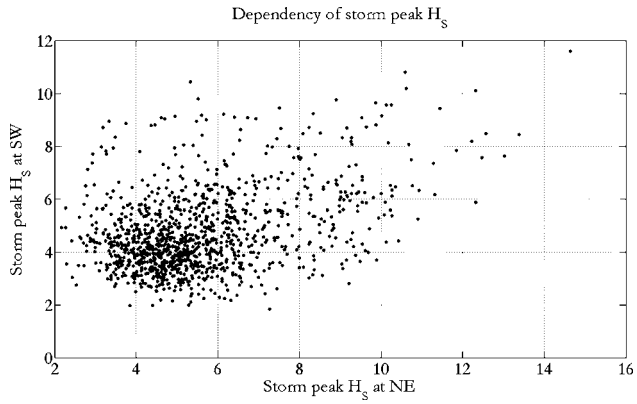

Fig. 4 Scatter plot of H_S^{sp} for NE location against SW. These locations give the lowest rank correlation between corner and center locations, but are nevertheless strongly interdependent.

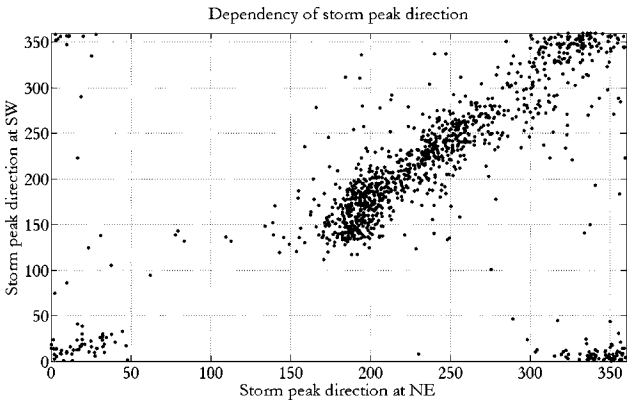

Fig. 6 Scatter plot of storm peak direction for NE location against SW. These locations give the largest median angular difference in storm peak direction from the corner and center locations, but are nevertheless strongly interdependent.

range of wave directions in general. Figure 7 gives the median directional dissipation ρ estimated using all storm data, as a function of H_S^{sp}. The directional dissipation of a storm is the minimum reduction in H_S (expressed as a fraction of H_S^{sp}) as a function of angular difference from the storm peak direction. For a given directional sector, therefore, the directional dissipation of a storm is the largest impact of that storm in that sector, expressed as a fraction of the storm peak H_S. For example, in Fig. 7, for a typical storm with H_S^{sp} above 14 m, the median directional dissipation at an angle of 30 deg is approximately 0.65. Therefore we would expect the maximum H_S associated with such a storm, for a direction 30 deg away from storm peak direction, to be approximately 0.65×14 m=9.1 m. For extreme value analysis in the peaks over threshold sense, we characterize a storm in terms of its storm peak significant wave height and storm peak direction only. However, in estimating directional design criteria, we also account for the influence of storms over their full range of sea states and wave directions, as will be described further in Secs. 3 and 4 below, using directional dissipation.

3 Extreme Value Modeling

3.1 Estimating the Extremal Threshold. Figures 1 and 2 above exhibit material changes in extremal behavior with direction. In particular, storm peaks with directions around [40,100) are smaller and less frequent than those with directions around [220,280). Nevertheless, to proceed with extreme value modeling, we need to specify an extremal threshold u. A fixed threshold, above which all storm peaks are taken to be "extreme," appropriate around [40,100) is unsuitable around [220,280). We might partition the data by direction and perform independent extreme value analyses per sector, assuming that sectors are effectively homogeneous. Here, alternatively, we adopt a threshold that varies with storm peak direction, thereby avoiding partitioning the data while accommodating directional heterogeneity. The variable threshold is estimated locally by identifying, for each storm peak present, the nearest 300 storm peaks in terms of storm peak direction. The variable threshold for that direction is then selected as a certain quantile q (e.g., the median, $q=0.5$) of H_S^{sp} for that sample of 300. The effect of varying the size of the local sample is to vary the smoothness of the estimated variable threshold profile with direction. The median was judged to provide a reasonable location for the onset of the extremal tail for all directions, as can be seen empirically from Fig. 1. For comparison, Fig. 8 gives the form of the variable threshold for $q=0.2$, $q=0.5$, and $q=0.8$. To check sensitivity to the choice of q, note that the complete analysis described here (in Secs. 3 and 4) for the median case was repeated

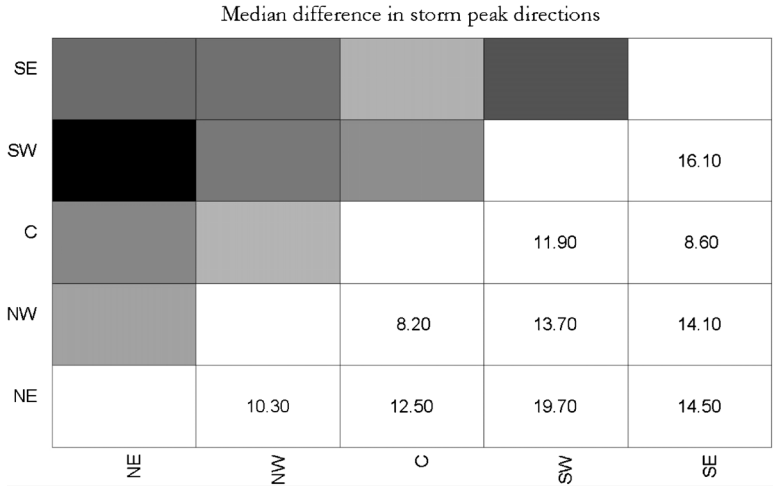

Fig. 5 Median differences (in degrees) between storm peak directions for corner and center locations. The top left illustrates difference on gray-scale (black=highest, white=lowest). The bottom right gives numeric values for median difference between pairs of locations.

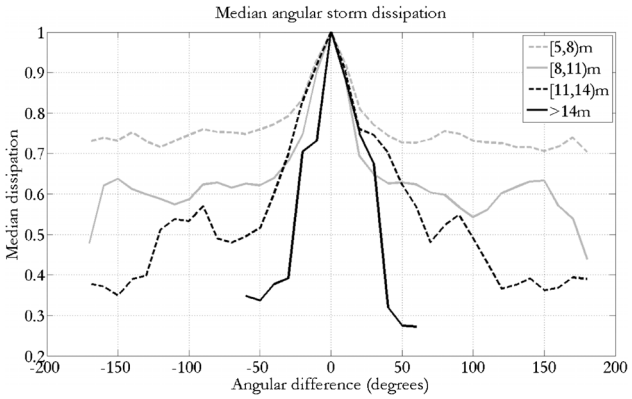

Fig. 7 Median directional storm dissipation ρ as a function of H_S^{sp}. For any storm, ρ is the minimum reduction in H_S (expressed as a fraction of H_S^{sp}) as a function of angular difference from the storm peak direction.

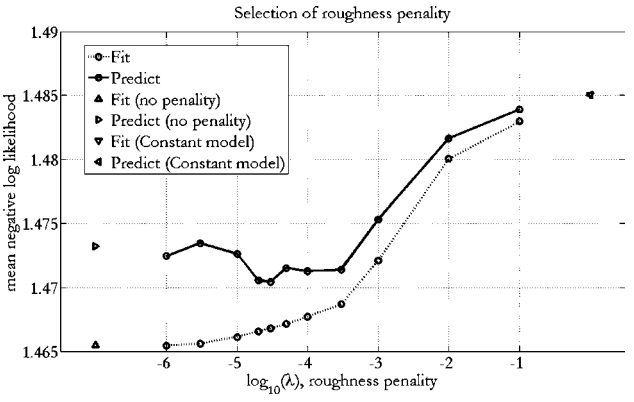

Fig. 9 Overall model fitting and prediction error as a function of λ. The optimal value for λ can be seen to be 3×10^{-5}. Note that points corresponding to fitting and predictive performance for the constant model are superimposed on the right-hand side.

for the case $q=0.2$; although differences were present in numerical values for model parameters, design values, etc., the key trends observed were consistent.

3.2 The Extreme Value Model. Given storm peak significant wave heights $\{X_i\}_{i=1}^n$ and storm directions $\{\theta_i\}_{i=1}^n$ (corresponding to a total of 100 different locations) occurring in some period P_0, we assume that for any storm the distribution of extreme wave heights above a certain threshold $u(\theta)$ can be described using the GPD with cumulative distribution function $F_{X_i|\theta_i,u}$ given by

$$F_{X_i|\theta_i,u}(x) = P(X_i \le x|\theta_i, u(\theta_i)) = 1 - \left(1 + \frac{\gamma(\theta_i)}{\sigma(\theta_i)}(x - u(\theta_i))\right)_+^{-1/\gamma(\theta_i)}$$

for $x > u, \sigma > 0$, where γ is the shape parameter or tail index, and σ is the scale. The subscript+notation, defined as $a_+ = \max(a, 0)$, is used. We expect the extreme value parameters γ and σ to vary smoothly with direction and characterize their directional dependence using a Fourier series expansion $\Sigma_{k=0}^{p}\Sigma_{b=1}^{2} A_{abk} t_b(k\theta)$, where $t_1 = \cos$, $t_2 = \sin$, with $a=1$ for γ, and $a=2$ for σ. We set $A_{a20}=0$, $a=1,2$ to avoid parameter redundancy. p is the order of the Fourier model, $p=0$ corresponding to a constant model. A Fourier form for γ and σ guarantees parameter estimates are periodic with respect to direction, and permits straight forward calculation of asymptotic covariances. The asymptotic covariance matrix of parameter estimates is given by the inverse I^{-1} of the information matrix, $I = E_X(\{-\partial^2 l / \partial A_{abk} \partial A_{\alpha\beta\kappa}\})$, where l is the log likelihood defined below. Asymptotic variances for functions of parameters, e.g., H_{S100}, can also be derived from I^{-1}. Asymptotic variances are useful as part of a bootstrapping resampling analysis to obtain reliable estimates for parameter uncertainties. The estimates $\hat{\gamma}$ and $\hat{\sigma}$ are intercorrelated, so that smoothing one functional form smoothes the other also [13]. Pooling dependent data samples (from the 100 locations) with the same extremal characteristics is advantageous since the sample size for modeling is increased. However, resulting asymptotic estimates for uncertainties of model parameters and design criteria are too small due to data dependency. Techniques such as bootstrapping are required to obtain realistic estimates of parameter uncertainties.

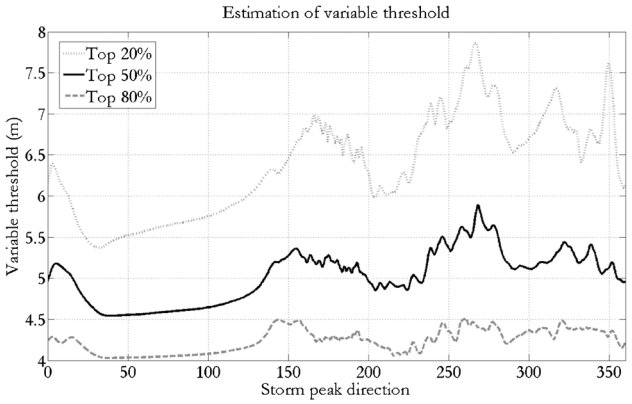

Fig. 8 Variable threshold estimates for local quantiles $q=0.2$, $q=0.5$, and $q=0.8$. The median case is adopted.

We estimate the parameters A_{abk}, $a=1,2$, $b=1,2$, $k=1,2,\ldots,p$ using roughness-penalized maximum likelihood estimation [17]. An order 10 model is judged to be sufficiently flexible to capture the directional dependence of γ and σ. A roughness term is incorporated for model fitting to penalize functional forms of γ and σ, which are not smooth. The penalized negative log likelihood to be maximized takes the form

$$l^*(\{A_{abk}\}; \{X_i\}_{i=1}^n) = \left(\sum_{i=1}^{n} l_i\right) - \lambda\left(R_\gamma + \frac{1}{w}R_\sigma\right)$$

Here, the unpenalized log likelihood, for $i=1,2,\ldots,n$ is

$$l_i = \log\sigma(\theta_i) + \left(\frac{1}{\gamma(\theta_i)} + 1\right)\log\left(1 + \frac{\gamma(\theta_i)}{\sigma(\theta_i)}(X_i - u(\theta_i))\right)_+$$

The roughness of γ is given by

$$R_\gamma = \int_0^{2\pi}\left(\frac{\partial^2\gamma}{\partial\theta^2}\right)^2 d\theta = \sum_{k=1}^{p} \pi k^4\left(\sum_{b=1}^{2} A_{1bk}^2\right)$$

The roughness of γ is given by

$$R_\sigma = \int_0^{2\pi}\left(\frac{\partial^2\sigma}{\partial\theta^2}\right)^2 d\theta = \sum_{k=1}^{p} \pi k^4\left(\sum_{b=1}^{2} A_{2bk}^2\right)$$

The constant w is set prior to modeling so that the ranges of values R_γ and $(1/w)R_\sigma$ are approximately equal. The value of the roughness parameter λ is selected using cross-validation [18] to maximize model predictive performance at locations not used for fitting as follows. Using a set of ten locations (on a 3×3 grid covering the region, with an additional near-central location added), models are fitted using data from nine locations only. The data from the remaining location are used to test how well the model works for prediction. This procedure is repeated until each location has been used exactly once for prediction, for a range of possible values of λ. Then we select that value of λ, which gives the best predictive performance across all locations. Figure 9 il-

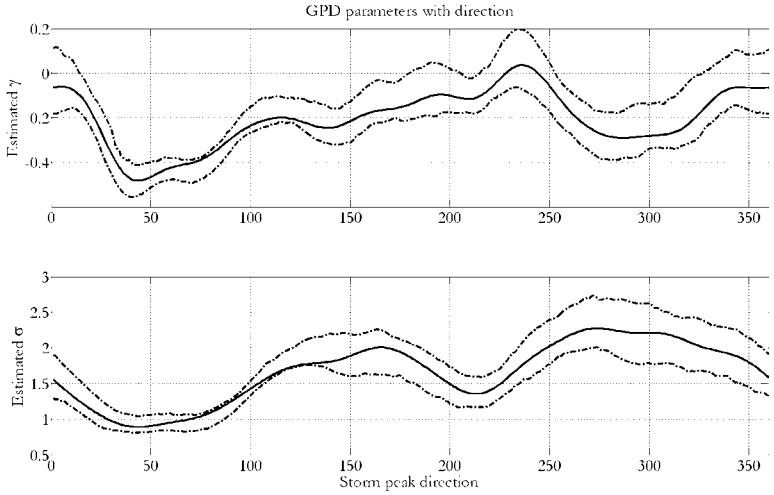

Fig. 10 The optimal functional forms of γ and σ, with bootstrap 95% confidence bands

lustrates overall model fitting error and predictive error as a function of λ. Model *fitting* error improves with decreasing λ, whereas the *predictive* error is minimized for $\lambda = 3 \times 10^{-5}$, at which predictive performance is optimal.

The corresponding functional forms of $\hat{\gamma}$ and $\hat{\sigma}$ with direction, evaluated using data for all storms at all locations with $\lambda = 3 \times 10^{-5}$, are shown in Fig. 10. The value of $\hat{\gamma}$ is seen to vary relatively smoothly from approximately −0.4 to above 0, indicating considerable heterogeneity in extremal behavior.

3.3 Estimating Parameter Uncertainty. As observed in Sec. 2 above, data from different locations are highly interdependent. Application of asymptotic estimators of uncertainty, appropriate for independent data samples, is inappropriate for samples obtained by aggregating dependent sites, and results in underestimation of uncertainty. Bootstrapping [19] is a more reliable approach to uncertainty estimation in such circumstances. Figure 10 shows 95% confidence bands for $\hat{\gamma}$ and $\hat{\sigma}$ with direction, estimated using the procedure described previously by the current authors [3] to directional modeling of Gulf of Mexico H_S^{sp} data.

3.4 Estimating H_{S100}. In any period P, the cumulative distribution function of the maximum storm peak H_S in any directional sector S is given by $F_{X\,\max_S}$ as follows:

$$F_{X\,\max_S}(x) = P(X_{\max\,S} \le x | X_i > u\ \forall\ i, i \in [1,2,\ldots,n]) = \prod_{i=1}^{n} \left\{ \sum_{k=0}^{\infty} P(\rho_i(S) X_i \le x | X_i > u_i, M_i = k) P(M_i = k) \right\}$$

where M_i is the number of occurrences of storm i in the period, the expected value of which is $m = P/P_0$ for all storms. $\rho_i(S)$ is the directional dissipation of storm i for the sector, equal to the *effective storm peak for storm i with respect to sector S*. Assuming M_i to be Poisson distributed, we have [13]

$$F_{X\,\max_S}(x) = \prod_{i=1}^{n} \left\{ \sum_{k=0}^{\infty} \left(1 - \left(1 + \frac{\gamma(\theta_i)}{\sigma(\theta_i)} \left(\frac{x}{\rho_i(S)} - u(\theta_i) \right) \right)_+^{-1/\gamma(\theta_i)} \right)^k \frac{e^{-m} m^k}{k!} \right\} = \prod_{i=1}^{n} \left\{ \exp\left\{ -m \left(1 + \frac{\gamma(\theta_i)}{\sigma(\theta_i)} \left(\frac{x}{\rho_i(S)} - u(\theta_i) \right) \right)_+^{-1/\gamma(\theta_i)} \right\} \right\}$$
$$= \exp\left\{ -m \sum_{i=1}^{n} \left(1 + \frac{\gamma(\theta_i)}{\sigma(\theta_i)} \left(\frac{x}{\rho_i(S)} - u(\theta_i) \right) \right)_+^{-1/\gamma(\theta_i)} \right\}$$

Using this approach, we calculate the median value of H_{S100} for a sequence of 36 consecutive directional sectors (each of width 10 deg partitioning the interval [0,360)) by solving $F_{X\,\max_S}(x) = 0.5$ for each sector S. The result is illustrated in Fig. 11 for a number of different scenarios. In the figure, the solid lines correspond to estimates for quantiles of sector H_{S100} using the order 10 directional model. The dashed lines correspond to estimates from a direction-independent model (order 0 constant, incorporating the variable extremal threshold) for comparison. The two gray curves correspond to median sector H_{S100} ignoring directional dissipation (light gray) and median sector H_{S100} with directional dissipation (dark gray). The black curve is the $0.98 (= 0.5^{1/36})$ quantile of sector H_{S100} with directional dissipation. If sectors were independent (which they are not because of directional dissipation), this sector quantile would be equivalent to median omnidirectional H_{S100}. Further, the median omnidirectional H_{S100} using the directional model is 15.8 m and the median omnidirectional H_{S100} using the constant model is 15.1 m.

From Fig. 11, we see that directional dissipation captures the effect on a sector of storms whose peaks lie outside the sector. Incorporating directional dissipation increases sector H_{S100}. Further, note that a constant (direction-independent) extreme value model, incorporating variable extremal threshold, underestimates median sector H_{S100} for sectors with large median sector H_{S100} and overestimates median sector H_{S100} for sectors with small median sector H_{S100}.

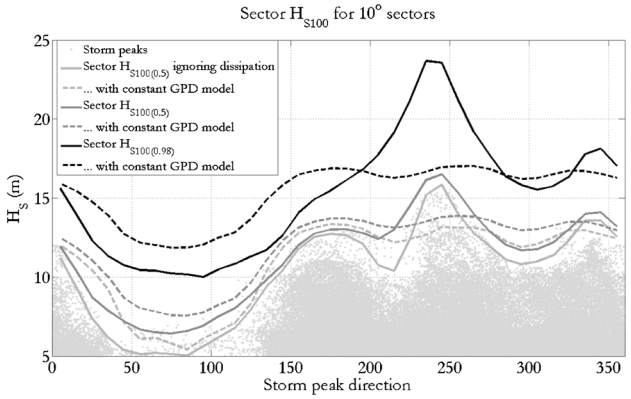

Fig. 11 Sector H_{S100} characteristics for a sequence of 36 consecutive directional sectors, each of width 10 deg, which partition [0,360), starting at 0 deg

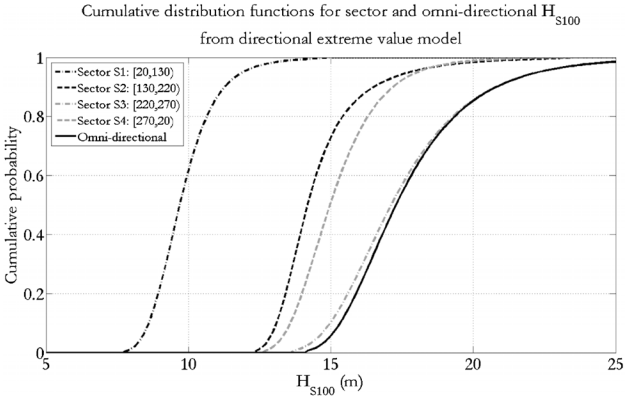

Fig. 13 Cumulative distribution functions for sector and omnidirectional H_{S100} using variable extremal threshold and directional model

4 Estimating Design Criteria

4.1 Selecting Directional Design Sectors. The directional variability of extremal behavior for the current locations suggests setting design criteria that also vary with direction. In literature [14], directional design criteria are quoted for directional sectors of fixed width 90 deg (or 45 deg) for appropriate orientations of the structure. However, in principle there is no requirement to define directional sectors of constant width. The selection of directional design sectors should reflect engineering requirements and constraints, and prevailing oceanographic conditions at the location. For the current application, we specify directional sectors that are as homogeneous as possible in terms of the 10 deg sector median H_{S100} discussed in Sec. 3 above. A simple iterative scheme is used to select that set of design sector boundaries that minimizes within-sector variability. Design sectors are constrained to be at least 45 deg in width, and the number of design sectors possible was limited to a maximum of 6, since this was anticipated, based on the exploratory analysis above, to be sufficient to characterize directional variability. The optimal four-design-sector solution is illustrated in Fig. 12 and is adopted for estimation of design criteria below.

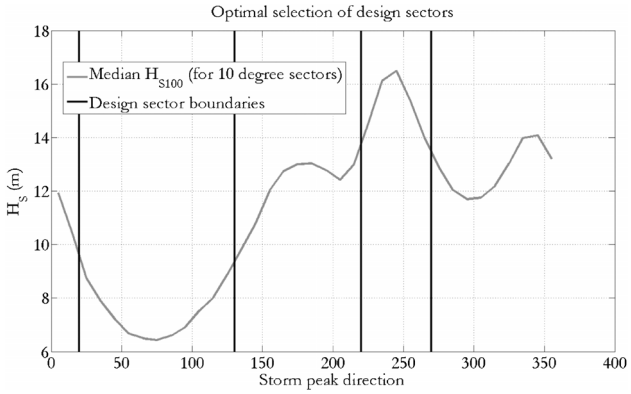

Fig. 12 Optimal boundaries for four directional design sectors

It is not surprising that the design sectors chosen by this method (see Table 1 below for angular specifications of sectors) reflect the main extremal characteristics at this location. The sectors correspond approximately to the shadow of Norway and the three long-fetch sectors, as can be seen from comparison with Figs. 1 and 2 in Sec. 2.

With this choice of directional design sectors, cumulative probability distribution functions for sector and omnidirectional H_{S100} were estimated using the procedure introduced in Sec. 3 above by solving $F_{X\,\max_S}(x)=q, q\in[0,1]$ for each sector S. The results are illustrated in Fig. 13 for the directional model. The dominant contributor to the omnidirectional cumulant (solid black line) is Sector 3, for storm peak directions in the interval [220,270). The difference between cumulants for Sectors 1 and 3 is noteworthy, as is the similarity of cumulants for Sectors 2 and 4.

Table 1 Design values corresponding to median omnidirectional storm peak H_{S100}, for the directional and constant models. Risk-cost, omnidirectional, and equal nonexceedence scenarios are evaluated.

Sector	Angle	Risk-cost optimal			Omnidirectional			Equal-nonexceedence probability		
Directional model		Risk cost	Value (m)	Quantile	Risk cost	Value (m)	Quantile	Risk cost	Value (m)	Quantile
S1	[20,130)	8.44	14.00	0.99	11.97	17.30	1.00	8.94	10.75	0.82
S2	[130,220)		15.50	0.81		17.30	0.94		15.58	0.82
S3	[220,270)		18.31	0.69		17.30	0.53		19.53	0.82
S4	[270,20)		16.40	0.81		17.30	0.91		16.44	0.82
Constant model		Risk cost	Value (m)	Quantile	Risk cost	Value (m)	Quantile	Risk cost	Value (m)	Quantile
S1	[20,130)	7.66	14.00	0.92	10.11	15.90	0.99	7.80	13.16	0.83
S2	[130,220)		16.08	0.80		15.90	0.76		16.20	0.83
S3	[220,270)		15.80	0.79		15.90	0.81		15.97	0.83
S4	[270,20)		16.06	0.80		15.90	0.76		16.21	0.83

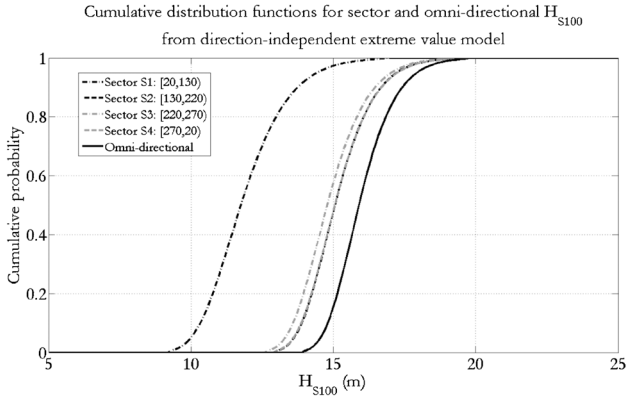

Fig. 14 Cumulative distribution functions for sector and omnidirectional H_{S100} using variable extremal threshold and direction-independent (constant) model

For comparison, Fig. 14 gives corresponding cumulants estimated using the order 0 constant model incorporating variable threshold. The difference in right-hand tails for the omnidirectional cumulants in Figs. 13 and 14 is considerable, due mainly to the underestimation of Sector 3 cumulant in Fig. 14. The cumulants for Sectors 2 and 4 are almost superimposed in Fig. 14.

4.2 Design Criteria. Using the estimates obtained above, we construct directional design criteria for the Northern North Sea location. We consider three different approaches, all consistent with the same given omnidirectional design criterion, in this case the median omnidirectional H_{S100}, and quantify their relative characteristics.

If design criteria are specified in terms of an omnidirectional nonexceedence probability $q_{100\text{omni}}$ for storm peak H_S, we obtain corresponding 100-year design storm peak H_S, $x_{100\text{omni}}$, by solving $q_{100\text{omni}}=P(X_{\max\ 100\text{omni}}\leq x_{100\text{omni}})$ However, specification of $q_{100\text{omni}}$ does not uniquely specify *sector* design storm peak H_S. Nevertheless, we can calculate sector nonexceedence probabilities $q_{100\text{omni}S_i}=P(X_{\max\ 100S_i}\leq x_{100\text{omni}})$ corresponding to $x_{100\text{omni}}$ for sectors $\{S_i\}_{i=1}^4$, and fix the value of the all-sector nonexceedence probability $\tilde{q}_{100\text{omni}}=\Pi_{i=1}^4 q_{100\text{omni}S_i}$ for all designs considered, to ensure consistency. Note that $\tilde{q}_{100\text{omni}}\neq q_{100\text{omni}}$ in general because of the influence of storms on multiple sectors due to directional dissipation [13]. Equality is achieved when each storm event influences one design sector only (which is actually approximately the case in the current application because of the judicious choice of sector boundaries above). This motivates the following three approaches to specification of directional design criteria.

4.2.1 Design to Omnidirectional H_{S100}. We design to the median omnidirectional storm peak H_{S100}, $x_{100\text{omni}}$, in all four sectors. Using this approach, since sectors exhibit different extremal behaviors the sector nonexceedence probabilities will vary. The all-sector nonexceedence probability will be $\tilde{q}_{100\text{omni}}$ as defined above.

4.2.2 Design to Equal Sector Nonexceedence. We design to the same nonexceedence probability $q_{100S_i}=(\tilde{q}_{100\text{omni}})^{1/4}$ in all four sectors $\{S_i\}_{i=1}^4$, thereby achieving the all-sector nonexceedence probability $\tilde{q}_{100\text{omni}}$, maintaining consistency with design to median omnidirectional storm peak H_S. Using this approach, since sectors exhibit different extremal behaviors the sector design values will vary.

4.2.3 Risk-Cost Optimal Design. To aid the selection of a balanced set of directional design criteria, we also take an intermediate approach, accommodating both design risk and cost, incorporating the aforementioned approaches as limiting cases. The so-called risk-cost optimal approach uses a design cost criterion to balance variability in sector design values and nonexceedence probabilities consistent with a given omnidirectional design criterion, in this case a given all-sector nonexceedence probability. The form of the expression for design cost is application specific. For definiteness here, we assume a design cost $RC=\frac{1}{100}\Sigma_{i=1}^4 c(x_{100S_i})$, where $c(x)=(x-14)_+^2$. That is, we penalize design values above 14 m with square penality, reflecting the additional cost of designing above this height. The factor $\frac{1}{100}$ is included purely for convenience. The risk-cost optimal design is that which minimizes RC given $\Pi_{i=1}^4 q_{100S_i}=\tilde{q}_{100\text{omni}}$.

The resulting directional sector design criteria are given in Table 1, for both the order 10 directional and the order 0 constant model. Comparing the top and bottom halves of the table, we see that design values based on the directional model are different from their counterparts obtained by analysis ignoring the directional dependence of storms. It has been shown theoretically [20] that given a sufficiently high threshold, the distribution of extremes over threshold converges in a certain sense to a generalized Pareto distribution, regardless of the underlying distribution of extremes. Therefore in our application, given a sufficiently high threshold for extreme value analysis, the omnidirectional extreme found from the directional model will be the same as that found from a conventional calculation (using the constant model ignoring directionality). This has been illustrated in a previous paper by the authors [15] using a simple two sector example (see Table 1 therein). However, in a typical application when directional effects are anticipated, such as the present case, the conventional estimation ignoring directionality may be unreliable, since the sample size available does not allow a sufficiently high threshold to be applied without unreasonably increasing the uncertainty of the estimate made. Any reduction in threshold (in order to increase the sample size) essentially contaminates the sample with measurements whose extremal properties are different from those of storm directions associated with the most extreme storms and thus biases omnidirectional estimates. Using the directional model, the smooth variation of extremal behavior with storm direction provides a more reliable basis for estimation. The model balances the flexibility required to explain the observed variation in extremal parameters, with the requirement that the variation in extremal parameters be as smooth as possible consistent with the data, thus reducing the effective number of degrees of freedom for model fitting. To demonstrate this effect further, a study is currently under way to compare estimates for omnidirectional extreme quantiles estimated using both the directional and conventional (constant) models with true values for simulated data with known directionally varying extremal structure.

The omnidirectional storm peak H_{S100} values for the directional model are larger. For the equal sector nonexceedence approach, the Sector 1 design value is smaller, and Sector 3 value larger for the directional model. These results indicate that ignoring directionality results in underestimation of extreme storms. Results also illustrate the different characteristics of the three design approaches used. The risk-cost optimal design reduces the range of nonexceedence probability values for design to omnidirectional, and reduces the range of storm peak H_S values for design to equal sector nonexceedence. Judging the risk-cost optimal design based on the directional model to be preferable, we conclude that we need to design for storm peak H_S of only 14 m in Sector 1, but for 18.3 m in Sector 3.

5 Conclusions and Recommendations

It is essential to capture directionality of extreme sea states when developing design criteria. Omnidirectional extreme values derived from a directional model can be materially different from a direction-independent derivation ignoring directional effects. In the current application, e.g., the omnidirectional storm peak H_{S100}

from a directional model is heavier tailed than that derived from a direction-independent approach, indicating that large values of storm peak H_S are more likely than we might anticipate were we to base our beliefs on estimates that ignore directionality. A directional extreme model allows directionally consistent extreme values to be developed. The case in favor of adopting a directional extreme value model is clear, unless it can be demonstrated statistically that a direction-independent model is no less appropriate. For the current application, a directional model characterizes the hindcast data significantly better than a conventional (direction-independent) model.

An extremal threshold, which varies with direction, is used to characterize the changing extremal properties of storm peak H_S with direction. A high-order Fourier form ensures that the directional extreme value model is sufficiently flexible to characterize variation in extremal behavior with storm direction. A roughness penality ensures that extreme value estimates are as smooth as possible consistent with the data within a maximum likelihood framework. Cross-validation is used to estimate the appropriate roughness penalty.

Extremal properties of storm peak H_S are modeled as a function of storm peak direction. Storm events are taken to be independent statistically for a given location. In estimating design criteria for a directional sector, we accommodate the effects of all sea states of all storms whose wave directions fall within that sector, regardless of the wave direction at storm peak, by quantifying the directional dissipation of every storm at every location and incorporating its influence on all directional sectors. In the current application, the rate of occurrence of storms peaks is dependent on storm peak direction. In general, distributions of storm peaks will be directionally dependent, even when extremal characteristics (e.g., GPD shape and scale) are independent of storm peak direction.

Directional design criteria provide more precise estimates of extreme offshore conditions enabling risk to be minimized given available resources. Yet directional design criteria are not uniquely defined given only an omnidirectional design criterion. We suggest a risk-cost criterion, which minimizes design cost for a given omnidirectional design specification, as an objective basis for estimation of directional criteria.

The availability of comprehensive metocean data allows the effect of the heterogeneity of extremes with respect to direction, season, and location to be accommodated in estimation of design criteria. This work is currently being extended to incorporate both directional and spatial variations in extremal behavior and design specification. We are also assessing the value of stratifying extremes sea states into wind-sea and swell components for directional analysis.

Acknowledgment

The authors acknowledge useful discussions with George Forristall and Michael Vogel, and thank Joost de Haan for his assistance with data handing. The authors further acknowledge the support of Shell International Exploration and Production and Shell Research Ltd.

References

[1] Elsinghorst, C., Groeneboom, P., Jonathan, P., Smulders, L., and Taylor, P., 1998, "Extreme Value Analysis of North Sea Storm Severity," ASME J. Offshore Mech. Arct. Eng., **120**, pp. 177–183.
[2] Forristall, G., Larrabee, R., and Mercier, R., 1991, "Combined Oceanographic Criteria for Deepwater Structures in the Gulf of Mexico," in *Proceedings Offshore Technology Conference*, Houston, TX.
[3] Jonathan, P., and Ewans, K. C., 2006, "Uncertainties in Extreme Wave Height Estimates for Hurricane Dominated Regions," in *Proceedings of the 25th International Conference on Offshore Mechanics and Arctic Engineering*, Hamburg, Germany, Jun. 4–8.
[4] Kotz, S., and Nadarajah, S., 2000, *Extreme Value Distributions: Theory and Applications*, Imperial College Press, London, UK.
[5] Reiss, R. D., and Thomas, M., 2001, *Statistical Analysis of Extreme Values*, Birkhauser, Basel, Switzerland.
[6] Coles, S., and Walshaw, D., 1994, "Directional Modelling of Extreme Wind Speeds," Appl. Stat., **43**, pp. 139–157.
[7] Robinson, M. E., and Tawn, J. A., 1997, "Statistics for Extreme Sea Currents," Appl. Stat., **46**, pp. 183–205.
[8] Coles, S. G., and Powel, E. A., 1996, "Bayesian Methods in Extreme Value Modelling: A Review and New Developments," Int. Statist. Rev., **64**, pp. 119–136.
[9] Coles, S. G., and Casson, E., 1998, "Extreme Value Modelling of Hurricane Wind Speeds," Struct. Safety, **20**, pp. 283–296.
[10] Casson, E., and Coles, S. G., 1999, "Spatial Regression Models for Extremes," Extremes, **1**, pp. 449–468.
[11] Coles, S. G., and Tawn, J. A., 1996, "A Bayesian Analysis of Extreme Rainfall Data," Appl. Stat., **45**, pp. 463–478.
[12] Coles, S. G., and Tawn, J. A., 2005, "Bayesian Modelling of Extreme Sea Surges on the UK East Coast," Philos. Trans. R. Soc. London, Ser. A, **363**, pp. 1387–1406.
[13] Ewans, K. C., and Jonathan, P., 2006, "The Effect of Directionality on Extreme Wave Design Criteria," in *Proceedings of the Ninth International Workshop on Wave Hindcasting and Forecasting*, Victoria, Canada, Sept. 24–29.
[14] Forristall, G. Z., 2004, "On the Use of Directional Wave Criteria," J. Waterway, Port, Coastal, Ocean Eng., **130**, pp. 272–275.
[15] Jonathan, P., and Ewans, K. C., 2008, "The Effect of Directionality on Extreme Wave Design Criteria," Ocean Eng., **34**, pp. 1977–1994.
[16] Oceanweather, 2002, North European Storm Study User Group Extension and Reanalysis Archive, Oceanweather Inc.; www.oceanweather.com
[17] Green, P. J., and Silverman, B., 1994, *Nonparametric Regression and Generalised Linear Models: A Roughness Penalty Approach*, Chapman and Hall, London, UK.
[18] Stone, M., 1974, "Cross-Validatory Choice and Assessment of Statistical Predictions," J. R. Stat. Soc. Ser. B (Methodol.), **36**, pp. 111–147.
[19] Davison, A. C., and Hinkley, D. A., 1997, *Bootstrap Methods and their Application (Cambridge Series in Statistical and Probabilistic Mathematics)*, Cambridge University Press, Cambridge, UK.
[20] Pickands, J., 1975, "Statistical Inference Using Extreme Order Statistics," Ann. Stat., **3**, pp. 119–131.